# Moisture Transport Associated with Southwest Monsoon Rainfall Over Sri Lanka in Relatively Wet and Dry Rainfall Years

**Sherly Shelton** ( sherly@mail.iap.ac.cn )
Institute of Atmospheric Physics Chinese Academy of Sciences

**Research Article**

**Keywords:** Southwest monsoon, wet and dry monsoon years, moisture flux, moisture convergence, Arabian Sea

**Posted Date:** November 29th, 2021

**DOI:** https://doi.org/10.21203/rs.3.rs-894605/v1

# Moisture Transport Associated with Southwest Monsoon Rainfall over Sri Lanka in relatively wet and dry rainfall years

Sherly Shelton[1,2,4*]

[1]*International Center for Climate and Environment Sciences, Institute of Atmospheric Physics, Chinese Academy of Sciences, P.O. Box 9804, Beijing 100029, China*

[2]*College of Earth and Planetary Sciences (CEPS), University of Chinese Academy of Sciences, Beijing 100049, China*

[3]*Industrial Technology Institute, Colombo, Sri Lanka*

[*] Corresponding Author: Email: sherly@mail.iap.ac.cn

***Abstract:*** Atmospheric moisture transportation associated with the occurrence of relatively wet and dry southwest monsoon (SWM) years over Sri Lanka is still not fully understood. This study focused on investigating the role of moisture transport in contrast SWM years. We selected seven wet ($SWM_{Wet}$) and nine dry ($SWM_{Dry}$) years for 1985-2015 and found that the whole country experiences above-average (below average) rainfall in $SWM_{Wet}$ ($SWM_{Dry}$) years. In $SWM_{Wet}$ years, strengthening moisture-laden low-level jets (LLJ) from the Arabian Sea bring a large amount of moisture towards Sri Lanka. In contrast, the weakening of the LLJ from the Arabian Sea direction is observed in $SWM_{Dry}$ years. As a consequence, the climatological mean of net moisture flux ($4.35 \times 10^5$ kg $s^{-1}$) over the study domain is increased ($5.33 \times 10^5$ kg $s^{-1}$) and decreased ($3.98 \times 10^5$ kg $s^{-1}$) in $SWM_{Wet}$ and $SWM_{Dry}$ years, respectively. With respect to long-term Vertically Integrate Moisture Flux Divergence (VIMFD, $-3.28 \times 10^{-5}$ kg $m^{-2}$ $s^{-1}$), negative anomalous VIMFD ($-1.78 \times 10^{-5}$ kg $m^{-2}$ $s^{-1}$) in $SWM_{Wet}$ years and positive anomalous VIMFD ($1.44 \times 10^{-5}$ kg $m^{-2}$ $s^{-1}$) in $SWM_{Dry}$ years are recorded, which ascribed above-average and below-average rainfall over the country. Furthermore, strong moisture convergence (divergence) center in the western/ southwestern part of Sri Lanka during the $SWM_{Wet}$ ($SWM_{Dry}$) years explain why strong positive and negative SWM rainfall anomalies are concentrated in these two regions. Furthermore, results highlighted a strong relationship between net moisture flux availability and SWM rainfall (r= 0.63) that may explain the observed SWM rainfall variability over the country.

***Keywords:*** Southwest monsoon, wet and dry monsoon years, moisture flux, moisture convergence, Arabian Sea

## 1. Introduction

According to Clausius–Clapeyron relation, moisture-holding capacity is increased by approximately 7% with degree temperature rise (Wasko et al. 2018), which implies that the ability to hold moisture in the atmosphere is increased under the warming climate. As a consequence, enhance moisture content in the atmosphere and continuous transport of huge amounts of water vapor and its associated convergence intensify the occurrence and of heavy rainfall events (Liu et al. 2020; O'Gorman 2015; Rayner and Chen 2010). For instance, Rajeevan et al. (2008) found that the increase of the extreme rainfall events over central India is directly associated with an increase in the moisture content due to the rapid warming of the equatorial Indian Ocean. On the other hand, less moisture transport for long periods and large horizontal moisture flux divergence are the main causes to occur drought (Held and Soden 2006). These prompt extreme rainfall events cause flooding landslides, soil erosion (Trenberth et al. 2003), and high streamflow (Neiman et al. 2013).

In tropical and subtropical regions, Low-level jet (LLJ) systems and atmospheric rivers (ARs) are two major mechanisms of atmospheric moisture transport. LLJs can be defined as the wind corridors of the lower atmosphere, which carry moisture transport from warm oceans toward continental areas or low to high latitudes (Gimeno et al. 2016). In the Indian subcontinent, the strengthening of monsoon LLJ brought large-scale advection of moisture is a prerequisite for heavy rainfall (Xavier et al. 2018). On the other hand, a decrease in the strength of cross-equatorial LLJ exists over the Indian Ocean is favourable for drought development (Joseph and Simon 2005). Based on these facts, wind convergence and water vapor advection by monsoon flow are playing a significant role in moisture convergence or divergence over the Indian monsoon region.

Southwest Monsoon (SWM) over the Indian monsoon region is generally termed as the Indian Summer Monsoon (ISM) (Dar and Ghosh 2017) and considered as one of the most active components of the climate system as part of the large-scale Asian monsoon (AM) circulation system (Kathayat et al. 2016). The availability of moisture transported from the warm waters of the Arabian Sea and Bay of Bengal (Turner and Annamalai 2012), high moisture convergence over the monsoon trough (Pathak et al. 2017), and the effects of topography (Konwar et al. 2012; Turner and Annamalai 2012) play a key role to originate the SWM rainfall over the landmass. Meanwhile, cross-equatorial moisture flux provides an important source of moisture for the SWM rainfall (Kathayat et al. 2016; Konwar et al. 2012; Ullah and Gao 2012). For instance, Roxy et al. (2017) quantify the total moisture contribution for extreme rainfall events in India and found that moisture comes from the Arabian Sea, the Bay of Bengal, and the central Indian Ocean contribute to 36%, 26%, and 9% of the, respectively. In addition, the moisture already in the atmosphere, and local surface evaporation, also contributing to SWM rainfall variability (Wang et al. 2017).

Rayner and Chen (2010) and Trenberth (1999) revealed that moisture contribution to the heavy and moderated rainfall events are associated with large distance transport, not from local evaporation. For example, during the strong monsoon years, SWM rainfall is characterized by stronger south-westerly LLJ, such as the Somali jet from the Arabian Sea, which directed more moisture into the Indian subcontinent between latitudes 5°N to 15°N. According to Joseph and Sijikumar (2004), the core of LLJ from the Arabian Sea has moved through 15° N during the active monsoon season. However, the LLJ has split into two branches during the break monsoon spell. The northern branch of the LLJ is at around 25° N, while the southern branch move moves south-eastward in the latitude belt from the 10°N to the equator (close to Sri Lanka). Based on these facts, the movement of the LLJ from the Arabian Sea has a different influence on SWM rainfall in Sri Lanka and the Indian

subcontinent. Interestingly we found that most of the floods and droughts are reported during the wet and dry SWM years, respectively. Therefore, the role of anomalies in the transport of moisture and moisture convergence/divergence during the contrast SWM years is helpful in understanding the causes of floods and droughts and of ongoing hydroclimate change.

Up to date, the role of moisture transport and the influence on this oceanic teleconnection with contrast SWM years over Sri Lanka is not well understood. Therefore, we have focused on identifying the abnormal water vapor transport pattern associated with moisture transport during the relatively wet and dry SWM years over Sri Lanka. The rest of the paper is organized as follows: Section 2 describes the general characteristics of the study area, data, and methodology. Section 3 is allocated for the result. Section 4 presents the discussion and conclusion of the study.

## 2. Study site, Data, and Methodology

### 2.1 Study Site

Sri Lanka is a tropical island country lying (5°55′~ 9°51′ N and 79°41′~ 81°53′ E) in the Indian Ocean and located in the path of the Indian monsoons circulation. The rainfall pattern in Sri Lanka is seasonally well distributed due to the movement of the intertropical convergence zone (ITCZ) over the equatorial region. As a result, seasonal variation in rainfall is strongly impacted by the southwest monsoon (SWM: June-September) and the northeast monsoon (NEM: December to February). In between two monsoon periods, the first inter-monsoon (FIM: March to May) and second inter-monsoon (SIM: October-November) seasons are identified (Malmgren et al. 2003). Three climatic zones are known as the wet zone, intermediate zone, and the semiarid dry zone, have been well-demarcated (Figure 1a) based on the regional differences in the amount of rain, seasonality, and variability (Rubasinghe et al. 2015). In addition, winds, temperature, relative humidity, and other

climatic elements also show significant differences between the three climate zones. The mean annual temperature in Sri Lanka demonstrates largely homogeneous temperatures in the lowlands. The mean annual average temperature is 27°C from the lowlands, up to an altitude of 100-150 m. The temperature is abruptly decreasing as the altitude increases in the highlands. For instance, the mean annual temperature at an altitude of about 1800 m is 15°C (Marambe et al. 2015).

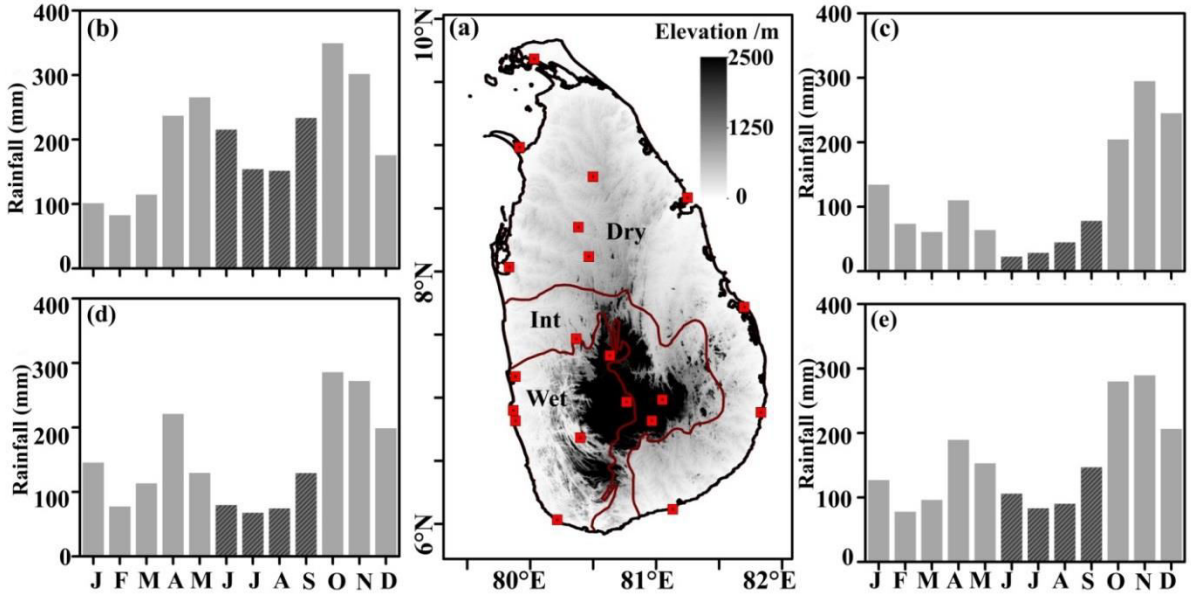


**Figure 1** (a) The spatial distribution of meteorological stations (red squares) on the topographic map of Lanka. The seasonal cycle of rainfall (unit: mm/month) for (b) wet, (c) dry (d) intermediate zones. (e) is same as (b) but for the whole country. The thick shaded bars represent the months belong to the southwest monsoon season (SWM; June – September).

## 2.2 Data

Monthly rainfall data for 20 metrological stations ranging from 1985 to 2015 were collected from the Department of Meteorology Sri Lanka. According to geographical distribution, 7, 3, and 10 metrological stations are located in the wet, intermediate, and dry climate zones, respectively (Figure 1a). In addition, GPCC V6 data set with 0.5° × 0.5° grid resolution were obtained from the Global Rainfall Climatology Centre (Schneider et al.

2011), covering the study period for investigating the spatial distribution of rainfall anomaly in contrasting SWM years. For reproducing and interpreting the atmospheric branch of the hydrological cycle, ERA-Interim (ERA-I) reanalysis data (Dee et al. 2011), more specifically, four times daily zonal and meridional wind, specific humidity, and surface pressure with 0.5° × 0.5° grid resolution data set have been used.

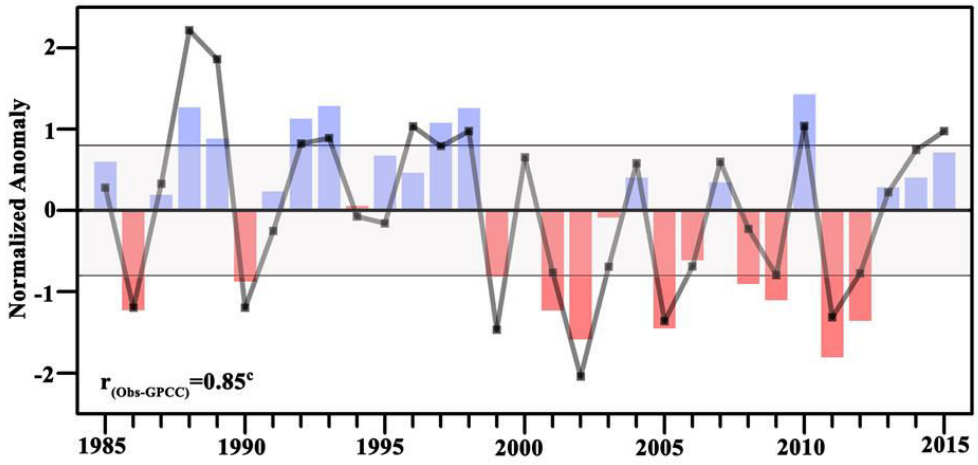


**Figure 2** Temporal evolution of normalized southwest monsoon (SWM) rainfall using station observation (bar graph) and GPCC data set (line graph) for the 1985-2015 period. The shaded strip depicts the selected threshold value (± 0.8) to select the set of $SWM_{Wet}$ and $SWM_{dry}$ years. The positive and negative normalized rainfall anomalies are shown in light blue and pink clour, respectively. The letter "c" indicates the statistically significant correlation ($r_{Obs\text{-}GPCC}$ ) between anomalous SWM rainfall from observation and GPCC at a 99% confidence level.

## 2.3 Methodology

In this study, we used composite sampling techniques for identifying the relatively wet and dry rainfall years. For this purpose, we first calculated area average rainfall using station-based observation using the Thiessen polygon (TP) method with the elevation regression method (Limin et al. 2015; Shelton and Lin 2019). Apart from that, we calculated

148 the area average SWM rainfall using the GPCC data. In the next stage, we derived
149 normalized anomalous SWM rainfall time series and applied it to identify relatively wet and
150 dry rainfall years, as follows. If the normalized SWM rainfall anomaly is above the +0.8, it
151 was identified as a relatively wet SWM (hereinafter $SWM_{Wet}$) year. In contrast, a relatively
152 dry SWM (hereinafter $SWM_{Dry}$) year is defined if the normalized anomaly is below –0.8
153 threshold levels in a particular year (Figure 2). Finally, eight wet and nine dry SWM years
154 were selected for further analysis (Table 1). Notably, we found that the SWM rainfall
155 anomaly from GPCC well produces the interannual variation of SWM rainfall in Sri Lanka
156 (Figure 2) with a high correlation coefficient ($r_{GPCC\text{-}Observed}$= 0.85). Therefore, we used GPCC
157 data to display the spatial rainfall climatology and anomalous rainfall distribution in $SWM_{Wet}$
158 and $SWM_{Dry}$ years.

159 **Table 1** The relatively wet ($SWM_{Wet}$) and dry ($SWM_{Dry}$) southwest monsoon(SWM)
160 years from 1985 to 2015.

| Season | Condition | Selected Year | | | | | | | | |
|---|---|---|---|---|---|---|---|---|---|---|
| **SWM** | $SWM_{Dry}$ | 1986 | 1990 | 1999 | 2001 | 2002 | 2005 | 2009 | 2011 | 2012 |
| | $SWM_{Wet}$ | 1988 | 1989 | 1992 | 1993 | 1997 | 1998 | 2010 | | |

161

162 In this study, the top layer of vertical integration is considered at 300 hPa because the
163 specific humidity above 300 hPa level is very low. According to (Ratna et al. 2016), moisture
164 transports above 300 hPa levels are a negligible influence on the calculation of Vertically
165 Integrated Moisture Flux (VIMF).

166 VIMF ($\vec{Q}$) in the troposphere from the surface to 300 hPa is calculated using *Eq.1*.

$$\vec{Q} = \frac{1}{g}\int_{300}^{Ps} q\,\vec{V}\,dp \ldots\ldots\ldots\ldots\ldots\ldots\ldots Eq.1$$

167 The zonal ($Q_\varphi$) and meridional($Q_\gamma$) components of the VIMF are calculated using Eq.2 and
168 Eq.3, respectively.

$$Q_\varphi = \frac{1}{g}\int_{300}^{Ps} qudp \ldots\ldots\ldots\ldots\ldots\ldots\ldots Eq.2$$

$$Q_\gamma = \frac{1}{g}\int_{300}^{Ps} qvdp \ldots\ldots\ldots\ldots\ldots\ldots\ldots Eq.3$$

169 Vertically Integrated Moisture Flux Divergence $\left(\mathrm{VIMFD};\nabla.\vec{Q}\right)$ was computed using *Eq.4*
170 (Trenberth and Guillemot 1998):

$$\nabla.\vec{Q} = \nabla.\frac{1}{g}\int_{300}^{Ps} q\,\vec{V}\,dp \ldots\ldots\ldots\ldots Eq.4$$

171 To understand the water vapor transports cross the four boundaries (*Fv*), Eastern
172 boundary: 5°N~10°N (at 82°E), western boundary: 5°N~10°N (at 79.5°E), southern
173 boundary: 79.5°E~82°E (at 5°N) and northern boundary: 79.5°E~82°E (at 10°N) were
174 defined, and the following equation (*Eq.5*) is used to calculate the moisture transport across a
175 wall.

$$Fv = \frac{1}{g}\int_{300}^{Ps}\int_{0}^{l} qVdp\,dl \ldots\ldots\ldots\ldots Eq.5$$

176 The vertical distribution of regional moisture fluxes via each lateral boundaries are calculated
177 as follow,

$$\vec{Q} = q \times \vec{V} \ldots\ldots\ldots\ldots\ldots Eq.6$$

178 Where *g, q, Ps,* $\vec{V}$*, u, v,* and *l* are the acceleration of gravity, specific humidity, surface
179 pressure horizontal wind vector, zonal wind, meridional wind, and a horizontal distance of
180 section, respectively. The regional moisture budget is calculated as the net effect of moisture

flux via each boundary. The positive regional moisture budget represented atmospheric water vapor transport from outside and converged within the region.

# 3 Results

## 3.1 Southwest Monsoon Rainfall in Sri Lanka

The seasonally varying monsoon system and the associated air masses and planetary wind regimes over South Asia have a great influence on the rainfall climate of Sri Lanka (Lin and Shelton 2020; Ranatunge et al. 2003). In this section, we take a closer look at the SWM rainfall contribution to annual total rainfall in different climate zones in Sri Lanka. As shown in Figure 1b, SWM rainfall contributes by 31.6% to the annual total rainfall (2382 mm) in the wet zone. For the intermediate zone, the annual total rainfall is 1974 mm, where it gets 19.3% during the SWM season (Figure 1d). The annual total rainfall in the dry zone is 1360 mm; out of that, 13% of rainfall receives from the SWM season (Figure 1c). When we consider the whole country average, the SWM rainfall contributes 23.1% to annual total rainfall (1845 mm) (Figure 1e). Furthermore, the spatial distribution of SWM rainfall climatology for 1985-2015 is shown in Figures 3a. As shown in Figure 3a, southwestern and southern parts of the country (wet zone) receive more rainfall from the SWM season. The observed spatial and temporal variability of SWM rainfall is associated with regional and local topographic influences. For instance, the central highlands of the country (Figure.1a) acts as an important physiographical climatic barrier that controls the prevailing moisture-laden monsoon winds by generating 'fohn effect weather conditions' among regions (Lin and Shelton 2020). Similarly, the South Asian monsoon is a fully coupled ocean-land-atmosphere system, which is also affected by fixed orography (Turner and Annamalai 2012). As an example, the contribution from the western Indian Ocean to the ISMR is limited due to the Western Ghats (Pathak et al. 2017), even most of the rainwater discharging during the IMSR is originated

over the ocean (Ordóñez et al. 2012). In addition, Shashikanth et al. (2014) revealed that the west coast and northeast India receive more precipitation during the summer monsoon because of the orographic effects of the Western Ghats and the Himalayas.

### 3.2 Monsoon rainfall distribution in relatively wet and dry years

In this section, we present the spatial distribution of anomalous rainfall distribution SWM during the two contrast monsoon years (Figures 3b-c). Notably, we found that the whole domain receives above-average rainfall in $SWM_{Wet}$ years, while large positive anomalous rainfall is more concentrated on the western and southwestern parts of the country (Figure 3b). According to the long-term climatological mean (1985-2015), the seasonal average SWM rainfall in the wet, intermediate, and dry climate zones is 188 mm, 89 mm, and 42 mm, respectively. We observed that the rainfall amount in wet, intermediate, and dry zones is increased by 21.2%, 24.1%, 22.5% during the $SWM_{Wet}$ years, respectively (Table 2). Figure 3c shows that the whole country experienced below-average rainfall during the $SWM_{Dry}$ years, while the western and southwestern parts of the country experienced more dry conditions than other regions. In contrast, the rainfall amount in wet, intermediate, and dry zones is decreased by 30.3%, 27.5%, and 35.5% in $SWM_{Dry}$ years, respectively (Table 2).

To identify the monthly rainfall variation in $SWM_{Wet}$ and $SWM_{Dry}$ years, we calculate the long-term mean (1985-2015) and mean for contrast monsoon years by using station based observation (Table 2). The long-term average rainfall for June, July, August, and September is 214.3, 154.5, 151.6, and 232.7 mm, respectively, which indicate that June and September are relatively wet as compared to other months in the SWM season. A similar observation is found for the intermediate zone; however, the dry zone receives more rainfall during August and September than the initial two months of the SWM season (Table 2).

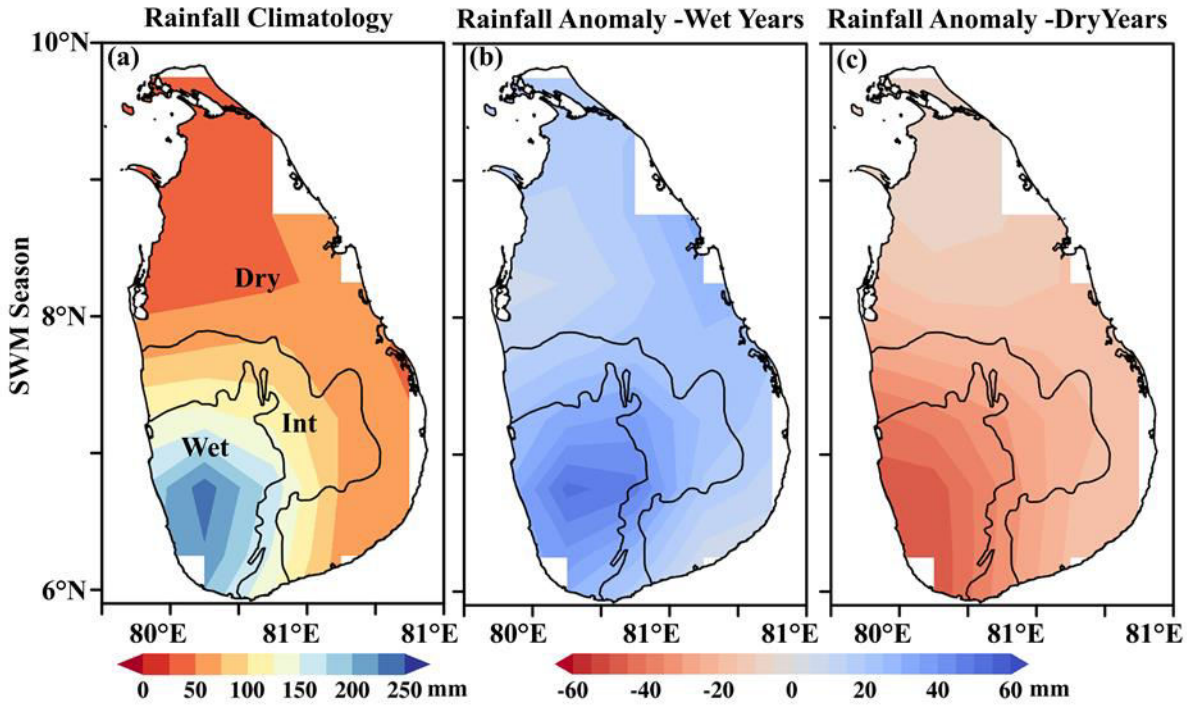


**Figure 3** Spatial distribution of southwest monsoon (SWM) rainfall (a) climatology (mm/month) from 1985 to 2015 and anomalous SWM rainfall (mm/month) for a set of relatively (b) wet and (c) dry SWM years. The wet, intermediate, and dry climate regions are demarcated by black lines and named as Wet, Int, and dry.

In $SWM_{Wet}$ years, the monthly mean rainfall over the wet zone increased by 22.2%, 39.5%, and 20.6% in June, July, and September, respectively. In contrast, all months of the season showed rainfall subsidence during the $SWM_{Dry}$ years, where the most considerable rainfall reduction is observed in June (32.2%) and September (34%) concerning the long-term mean value of the monthly rainfall. Similarly, results show that both dry and intermediate zones show a percentage increase (decrease) in monthly rainfall for $SWM_{Wet}$ ($SWM_{Dry}$) years. For instance, in $SWM_{Wet}$ years, the July rainfall is increased by 70.8% over the intermediate and 85.2 % over dry zones, respectively. In contrast, the largest rainfall subsidence over intermediate and dry zones is observed June (45.9%) and July (42.0%) (Table 2).

**Table 2** The monthly and seasonal average rainfall for the long-term climatology(mm), and percentage change (%) of the rainfall from the long-term mean value for relatively wet ($SWM_{Wet}$) and dry SWM ($SWM_{Dry}$) years. The Wet, Int, and Dry denote three climate zones in Sri Lanka.

| Zones | Condition | June | July | August | September | SWM |
|---|---|---|---|---|---|---|
| **Wet** | Average (mm) | 214.3 | 154.5 | 151.6 | 232.7 | 188.3 |
| | $SWM_{Wet}$ (%) | 22.2 | 39.5 | 2.2 | 20.6 | 21.2 |
| | $SWM_{Dry}$ (%) | -32.4 | -25.5 | -26.4 | -34.1 | -30.3 |
| **Int** | Average (mm) | 80.9 | 72.1 | 74.7 | 129.2 | 89.2 |
| | $SWM_{Wet}$ (%) | 21.0 | 70.8 | 18.7 | 3.0 | 24.1 |
| | $SWM_{Dry}$ (%) | -45.9 | -17.7 | -13.4 | -29.7 | -27.5 |
| **Dry** | Average (mm) | 26.4 | 25.6 | 43.9 | 73.8 | 42.4 |
| | $SWM_{Wet}$ (%) | 3.9 | 85.2 | 22.0 | 7.7 | 22.5 |
| | $SWM_{Dry}$ (%) | -35.4 | -42.0 | -22.9 | -40.4 | -35.3 |

Meanwhile, we investigate spatial variation of rainfall in months of the SWM season. Figures 4a-d show the spatial distribution of rainfall climatology (1985-2015) for June, July, August, and September, while the middle (Figures 4a1-d1) and lower (Figures 4a2-d2) panels depict the anomalous rainfall in each month for $SWM_{Wet}$ and $SWM_{Dry}$ years, respectively. Notably, we found that all the months of the SWM season bring a considerable amount of rainfall over the wet zone, where the rainfall peaks are observed in June and September. In general, the intermediate and dry zones receive less than 100 mm rainfall in individual months of the season except for September (Figures 4a-d).

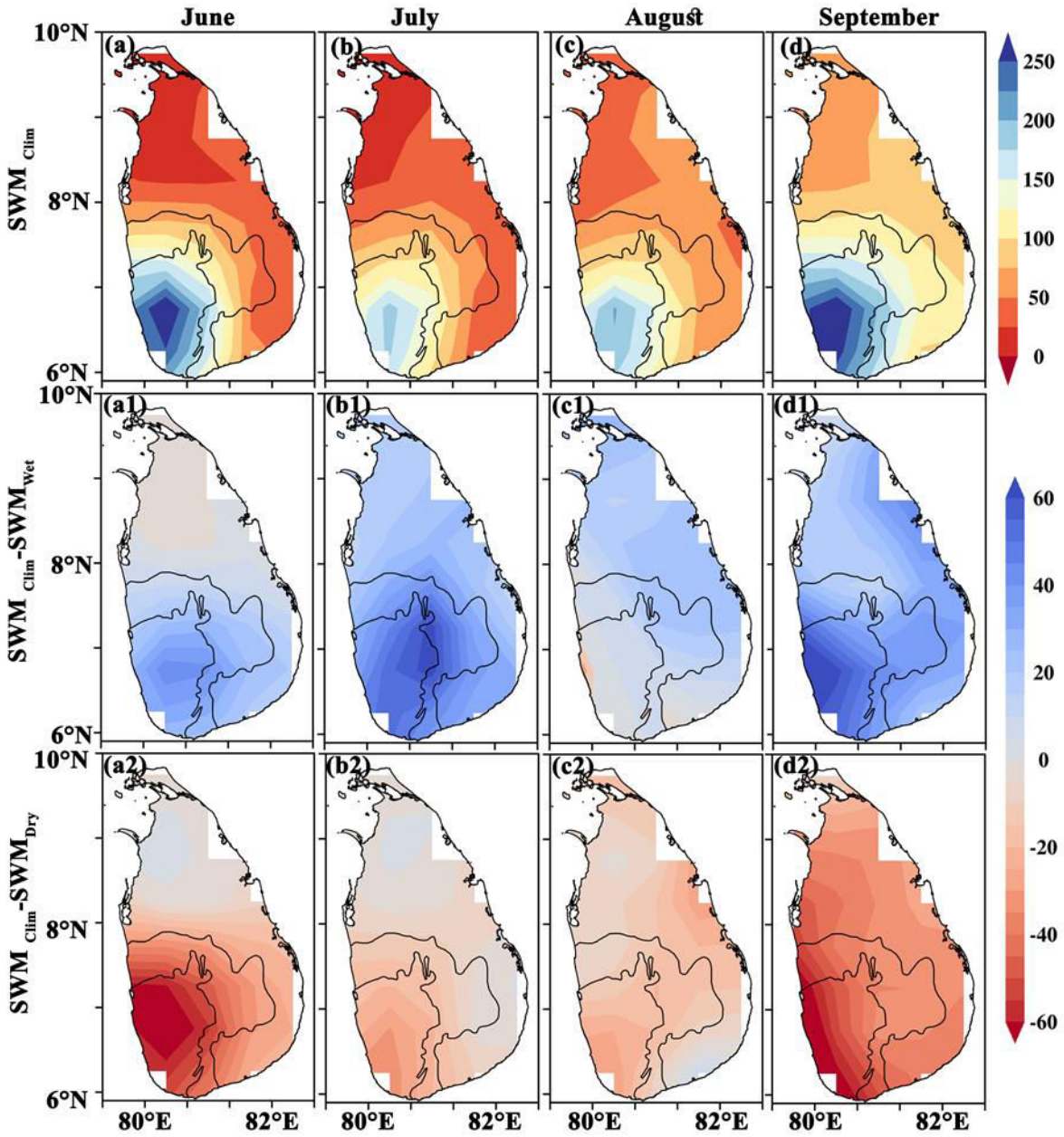


259

260 **Figure 4** Spatial distribution of rainfall (unit; mm) for a long-term average ($SWM_{Clim}$;
261 1985-2015) of the (a) June, (b) July, (c) August, and (d) September. The middle (a1-d1) and
262 right (a2-d2) columns are the same as the left column but for the anomalous rainfall for
263 relatively (b) wet ($SWM_{Wet}$) and (c) dry SWM ($SWM_{Dry}$) years.

264 During $SWM_{Wet}$ years, all months of the season showed above-average rainfall, while
265 strong positive anomalous rainfall is observed in July and September. The other remarkable
266 feature of Figures 4a1-d1 is most of the positive anomalous rainfall is concentrated in the wet

zone except August in the SWM season. In $SWM_{Dry}$ years, strong negative anomalous rainfall is observed in June and September, while it is localized to the wet zone (Figures 4a2-d2). In order to investigate the possible reason for the above-average and below-average rainfall in the SWM season, the moisture transports and associated moisture flux divergence/convergence in $SWM_{Wet}$ and $SWM_{Dry}$ years have been analyzed in the next section.

### 3.3 Vertically Integrated Moisture Flux and its Divergence

According to Trenberth et al. (2003) and Gao and Sun (2016), the ascending motion, the microphysics inside cloud droplets, and moisture supply determine whether rainfalls or not in a particular region. It is noticed that the large-scale convergence rather than locally enhanced evaporation controls the precipitation patterns in the tropics (Allan and Soden 2007; Trenberth et al. 2003). Therefore, analysis of the moisture transport and its divergence/ convergence provides insights into the major modes of precipitation variability over the country, as well as the moisture sources themselves. Therefore, climatological vertical integrated moisture flux (VIMF; vector) over Sri Lanka is investigated to understand the water vapor supply towards the country in the SWM season (Figures 5a). In the same figure, we display the climatological vertically integrated moisture flux divergence (VIMFD; shaded).

As shown in figure 5a, the VIMF vector from the Arabian Sea direction supplied moisture towards the convention center over Sri Lanka. Similarly, Pathak et al. (2017) found that moisture flux from the Western Indian Ocean (Arabian Sea) direction is the most important contributor for the initial phase of the Indian monsoon as compared to moisture flux from south of the equator direction. In the same study, they identify the regions with high vertically integrated moisture flux divergence as the potential sources of atmospheric moisture; meanwhile, regions with high convergence are considered as potential sink regions.

Figure 5a also shows climatological mean moisture flux divergence (+ value) over the Arabian Sea direction (source) as well as the Bay of Bengal, while more moisture convergence (– divergence) over the western and southwestern parts (sink) of the county during the SWM season. We further notice strong moisture divergence over the eastern and southeastern parts of the country.

In Figure 5b, we show the anomalous water vapor fluxes (vectors) and associated moisture flux divergence (shaded) for the $SWM_{Wet}$ years. Compared to the mean state, the excess moisture fluxes can be seen over the study region, and vectors move towards the South Indian sea direction. Furthermore, we detected cyclonic circulation of the VIMF over the Bay of Bengal and the northeastern part of the Arabian Sea during $SWM_{Wet}$ years, which inject moisture-laden wind towards the country. In contrast, the weakening of the westerly transport moisture flux can be observed over Sri Lanka and most of the eastern part of the Arabian Sea during $SWM_{Dry}$ years (Figure 5c), which results in less moisture availability and ultimately it caused SWM rainfall subsidence over Sri Lanka. Similar to our findings, Ratna et al. (2014) found that the weakening of westerlies reduced the moisture transport towards the southern part of the Western Ghats as well as local precipitation over India. Levine and Turner (2012) also pointed out that the strongest monsoon in the Indian subcontinent depended heavily on the moisture flux of the Arabian Sea.

Furthermore, we observed considerable spatial variations in the anomalous moisture flux divergence during the $SWM_{Wet}$ and $SWM_{Dry}$ years over Sri Lanka (Figure 5b-c). For instance, an area with negative anomalous divergence has been observed over the western and southwestern parts of the country, while negative moisture flux divergence is observed over Western Ghats and Bay of Bengal as well in $SWM_{Wet}$ years (Figure 5b). In $SWM_{Dry}$ years, all the study domain depicts positive divergence fluxes anomaly, while strong divergence centers are located over the western and southwestern parts of the country.

Meanwhile, we further observed positive anomalous moisture flux divergence over the Bay of Bengal (Figure 5c). A closer look at the anomalous moisture divergence over Sri Lanka suggests that SWM rainfall is mostly concentrated over the western and southwestern parts of the country, which is attributed due to the influence of the central mountain of Sri Lanka. As a result, western and southwestern parts receive more (less) rainfall in $SWM_{Wet}$ ($SWM_{Dry}$) years.

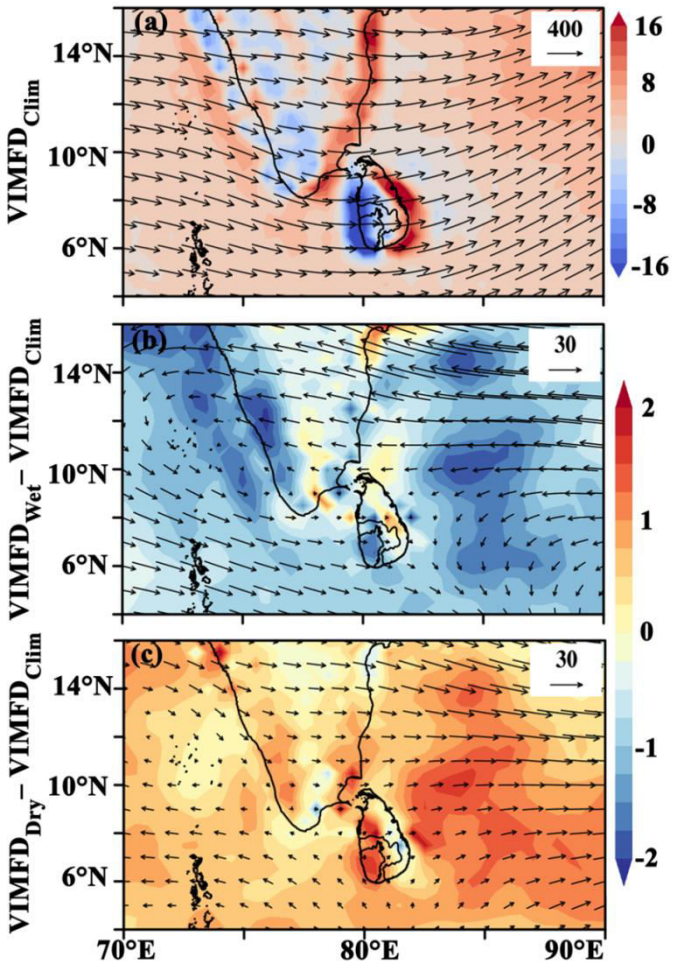


**Figure 5** Vertically integrated moisture flux divergence (VIMFD, shaded, unit; $10^{-6}$ kg $m^{-2}$ $s^{-1}$) superimposed with vertically integrated moisture flux (VIMF, vector, unit: kg $m^{-1}$ $s^{-1}$) for (a) a long-term average of the southwest monsoon season ($VIMFD_{Clim}$) and anomalies for relatively (b) wet ($SWM_{Wet}$) and (c) dry SWM ($SWM_{Dry}$) years.

329 On the other hand, we have taken a closer look at monthly moisture flux and its
330 convergence/divergence over the study domain during the $SWM_{Wet}$ and $SWM_{Dry}$ years
331 (Figure 6). As shown in Figure 6a-d, the moisture flux from the Arabian sea direction moves
332 through Sri Lanka towards the Bay of Bengal direction in all the months of the SWM season
333 (June-September), while the strong moisture fluxes (vectors) is observed in June. Another
334 remarkable feature we observed in this figure is strong moisture flux convergence over the
335 western/southwestern parts and moisture divergence in the northeast and east parts of the
336 country. The climatological VIMFD further shows that no significant difference in VIMFD
337 among the month of the SWM season.

338 When we consider the VIMF anomaly in $SWM_{Wet}$ years, all the months except
339 August show above-average VIMF, while cyclonic circulation of VIMF is observed over the
340 Arabian sea direction in June**.** In the $SWM_{Wet}$ years, the strong moisture flux convergence is
341 observed near the Western Ghats and over the Bay of Bengal during the first two months of
342 the season. Furthermore, we detected that strong moisture flux convergence over the
343 south/southwestern parts of Sri Lanka in June, July, and September (Figures 6a1-b1 and d1),
344 while the moisture flux convergence in August is less as compared with other months of the
345 seasons (Figure 6c1).

346 In $SWM_{Dry}$ years, we observe that the strength of the VIMF is reduced from June-
347 September. As shown in Figures 6a2-c2, the strong moisture flux divergence is located over
348 the Bay of Bengal in June, which is gradually decreasing up to August. Furthermore, we
349 detected strong moisture flux divergence over the south/southwestern parts of Sri Lanka in
350 $SWM_{Dry}$ years, especially in September, where divergence is stronger than the other three
351 months of the season (Figure 6d2)**.**

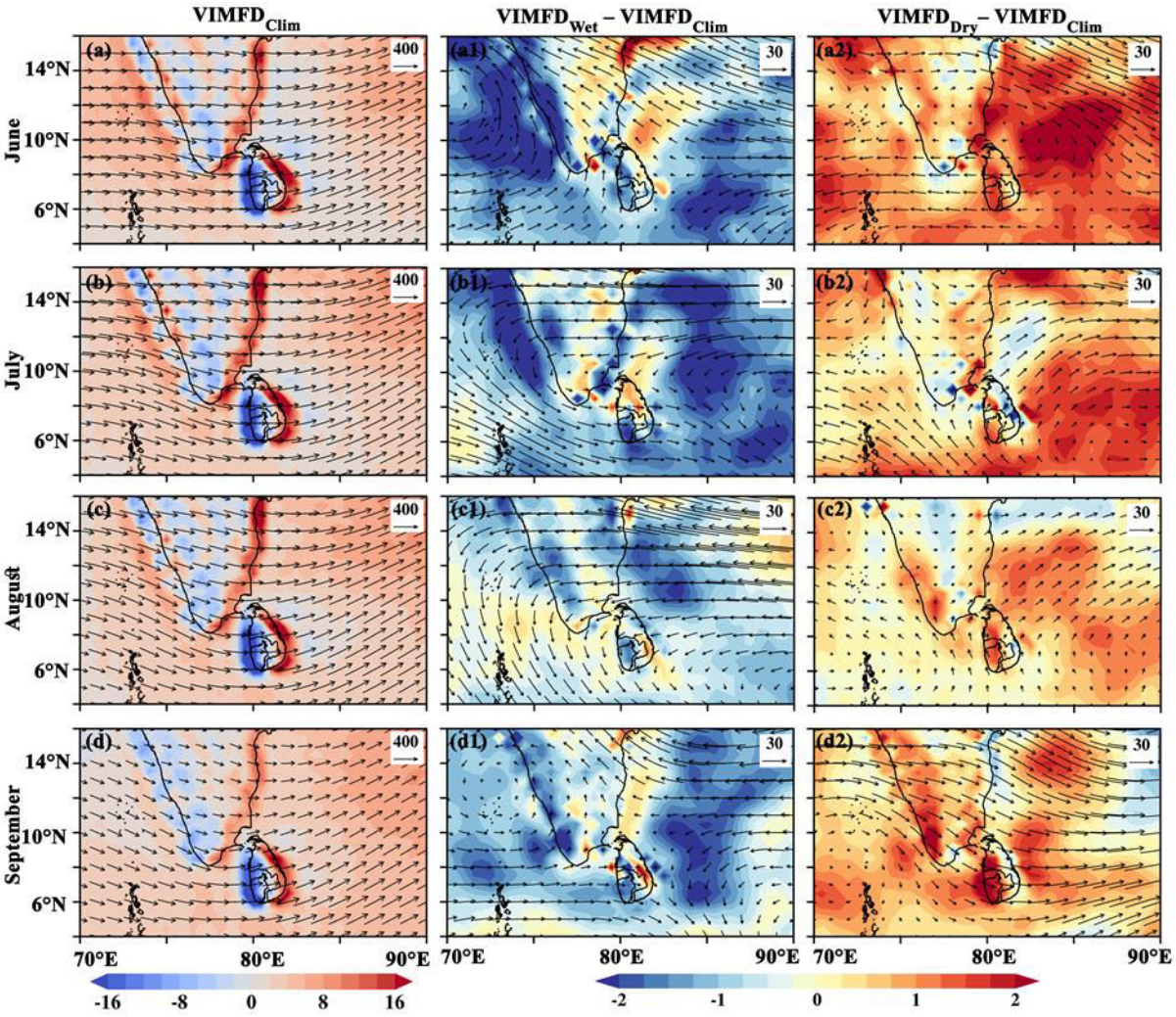


**Figure 6** Vertically integrated moisture flux divergence (VIMFD, shaded, unit; $10^{-6}$ kg $m^{-2}$ $s^{-1}$) superimposed with vertically integrated moisture flux (VIMF, vector, unit: kg $m^{-1}$ $s^{-1}$) for a long-term average (1985-2015) of the (a) June, (b) July, (c) August, and (d) September. The middle (a1-d1) and right (a2-d2) columns are the same as the left column but for the anomalous VIMFD and VIMF for relatively (b) wet ($SWM_{Wet}$) and (c) dry SWM ($SWM_{Dry}$) years.

### 3.4 Moisture Flux Through Different Boundaries

In this section, we quantify the moisture transport via different boundaries and investigate the anomalous moisture flux in $SWM_{Wet}$ and $SWM_{Dry}$ years. In addition, The regional average net moisture flux is calculating by getting the difference of moisture influx

and outflux from the different boundaries of the study domain. The long-term climatology of moisture transport from each boundary and associated anomalous moisture fluxes for $SWM_{Wet}$ and $SWM_{Dry}$ years are depicted in Figures 7a-c. Based on the long-term climatology for moisture fluxes for SWM season, the western ($20.36\times10^5$ kg $s^{-1}$) and southern ($14.60\times10^5$ kg $s^{-1}$) boundaries act as moisture influx boundaries, while eastern ($19.86\times10^5$ kg $s^{-1}$) and northern ($10.69\times10^5$ kg $s^{-1}$) boundaries are considered as the main moisture outflux boundaries (Figure 7a).

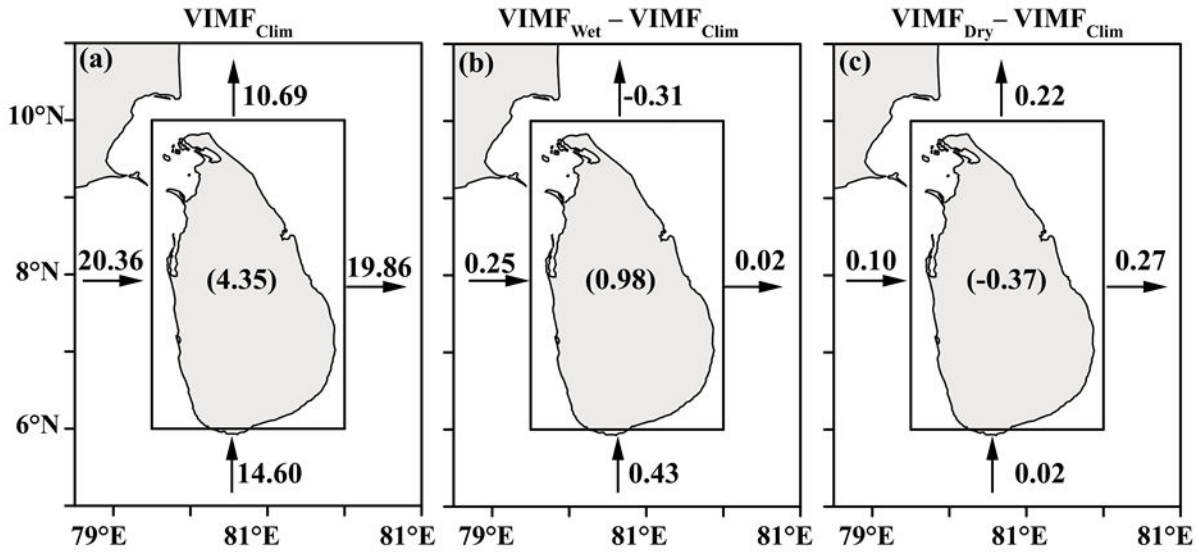


**Figure 7** The vertically integrated moisture flux (VIMF) across the four different boundaries for (a) a long-term average of the southwest monsoon season ($VIMF_{Clim}$), and anomalies for relatively (b) wet ($SWM_{Wet}$) and (c) dry SWM ($SWM_{Dry}$) years. Dark arrows indicate the climatological direction of the moisture transport across the wall. The number in brackets indicates the net flux convergence (unit: $10^5$ kg $s^{-1}$). The inner box shows the western (6°N~10°N at 79.5°E), eastern (6°N~10°N at 82°E), southern (79.5°E~82°E at 6°N) and northern (79.5°E ~82°E at 10° N) boundaries.

The anomalous moisture influx from the western and southern boundary during the $SWM_{Wet}$ years is $0.25\times10^5$ and $0.43\times10^5$ kg $s^{-1}$, respectively. However, the amount of moisture influx decreased during the $SWM_{Dry}$ years; for instance, the influx anomaly for the western boundary is $0.10\times10^5$ kg $s^{-1}$ and $0.02\times10^5$ kg $s^{-1}$ for the southern boundary. As a moisture outflux boundary, the eastern boundary reported $0.02\times10^5$ kg $s^{-1}$ and $0.27\times10^5$ kg $s^{-1}$ anomalous moisture flux for the $SWM_{Wet}$ and $SWM_{Dry}$ years, respectively. At the same time, moisture outflux through the northern boundary showed a negative anomaly ($-0.31\times10^5$ kg $s^{-1}$) during the $SWM_{Wet}$ years, while the positive anomaly ($0.22\times10^5$ kg $s^{-1}$) is observed in $SWM_{Dry}$ years (Figures 7b-c). Similar to our findings, Ratna et al. (2014) found the main moisture influx and outflux for the Indian subcontinent are the southern boundaries of the Arabian Sea and the eastern boundary, respectively. Considering the moisture influx and outflux, the area-average net moisture budget (hereinafter, NetMB) for the 1985-2015 period over the study domain is $4.35\times10^5$ kg $s^{-1}$. Figures 7b-c further show the positive NetMB anomaly ($0.98\times10^5$ kg $s^{-1}$) and negative NetMB anomaly ($-0.37\times10^5$ kg $s^{-1}$) in $SWM_{Wet}$ and $SWM_{Dry}$ years, respectively.

Based on the results, we can explain the observed rainfall variability in relatively wet and dry monsoon years in terms of net moisture flux over the study domain. For instance, positive NetMB is one of the reasons for the relatively wet monsoon rainfall events over Sri Lanka. To further prove this, the relationship between seasonal rainfall anomalies over Sri Lanka and NetMB has been evaluated, as shown in Figures 8. For the SWM season, the normalized NetMB shows a statistically significant correlation with the normalized SWM rainfall anomaly calculated using station based observation (r= 0.63) and GPCC product (r= 0.59) (Figure 8).

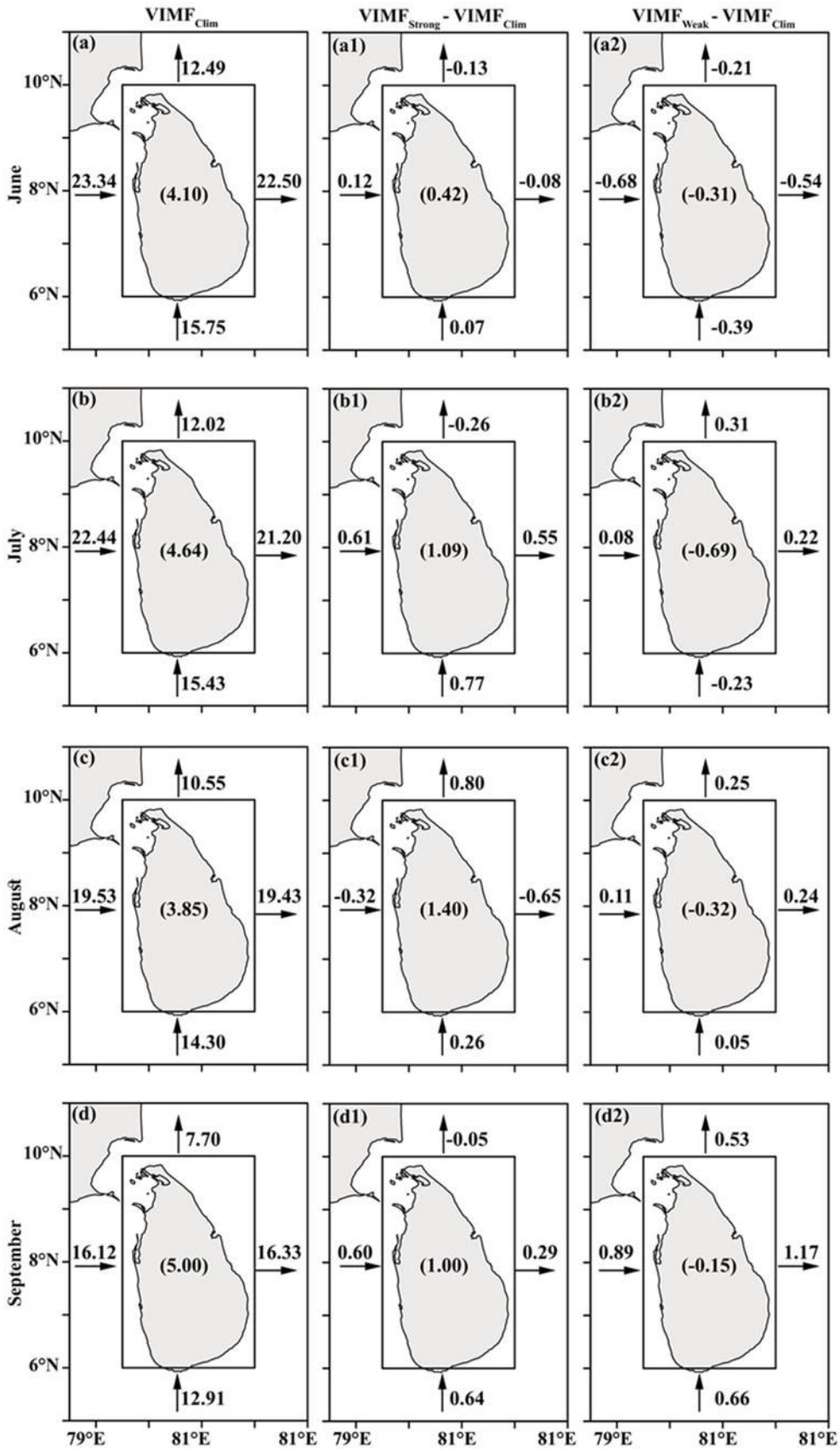
VIMF$_{Clim}$
VIMF$_{Strong}$ - VIMF$_{Clim}$
VIMF$_{Weak}$ - VIMF$_{Clim}$
(a)
12.49
23.34
(4.10)
22.50
15.75
(a1)
-0.13
0.12
(0.42)
-0.08
0.07
(a2)
-0.21
-0.68
(-0.31)
-0.54
-0.39
June
(b)
12.02
22.44
(4.64)
21.20
15.43
(b1)
-0.26
0.61
(1.09)
0.55
0.77
(b2)
0.31
0.08
(-0.69)
0.22
-0.23
July
(c)
10.55
19.53
(3.85)
19.43
14.30
(c1)
0.80
-0.32
(1.40)
-0.65
0.26
(c2)
0.25
0.11
(-0.32)
0.24
0.05
August
(d)
7.70
16.12
(5.00)
16.33
12.91
(d1)
-0.05
0.60
(1.00)
0.29
0.64
(d2)
0.53
0.89
(-0.15)
1.17
0.66
September
10°N
8°N
6°N
79°E
81°E

402

**Figure 8** The vertically integrated moisture flux (VIMF) across the four different boundaries in Sri Lanka for a long-term average of (a) June, (b) July, (c) August, and (d) September. The middle (a1-d1) and right (a2-d2) panels are the same as left panels but for the VIMF anomalies for relatively wet ($SWM_{Wet}$) and dry SWM ($SWM_{Dry}$) years, respectively. Dark arrows indicate the climatological direction of the moisture transport across the wall. The number in brackets indicates the net flux convergence (unit: $10^5$ kg $s^{-1}$). The inner box shows the western (6°N~10°N at 79.5°E), eastern (6°N~10°N at 82°E), southern(79.5°E~82°E at 6°N), and northern(79.5°E ~82°E at 10° N) boundaries.

We further analyze the NetMB in each month of the season, as depicted in Figure 9. The long-term climatology of the NetMB in June, July, August, and September are $4.10\times10^5$ kg $s^{-1}$, $4.64\times10^5$ kg $s^{-1}$, $3.85\times10^5$ kg $s^{-1}$, and $5.00\times10^5$ kg $s^{-1}$, respectively (Figure 9a-d). Interestingly, we found that the western boundary is the main moisture influx in all the months. For instance, the large moisture influx via the western boundary is recorded in June ($23.34\times10^5$ kg $s^{-1}$), which is gradually decreasing with time (e.g., $16.12\times10^5$ kg $s^{-1}$ in September).on the other hand southern boundary also act as moisture influx where the highest and lowest influxes are recorded in June ($15.75\times10^5$ kg $s^{-1}$) and September ($12.91\times10^5$ kg $s^{-1}$) respectively. In terms of magnitude, the eastern boundary act as a major outflux boundary for each month of the SWM season. Similar to the influx boundary, the outflux from the eastern boundary is decreasing with time; for instance, the outflux in June is $22.50\times10^5$ kg $s^{-1}$, which decreased up to $16.33\times10^5$ kg $s^{-1}$ in September. The northern boundary also acts as the outflux boundary where the largest outflux is recorded in June ($12.49\times10^5$ kg $s^{-1}$), while the lowest outflux ($7.70\times10^5$ kg $s^{-1}$) is detected in September (Figure 9a-d).

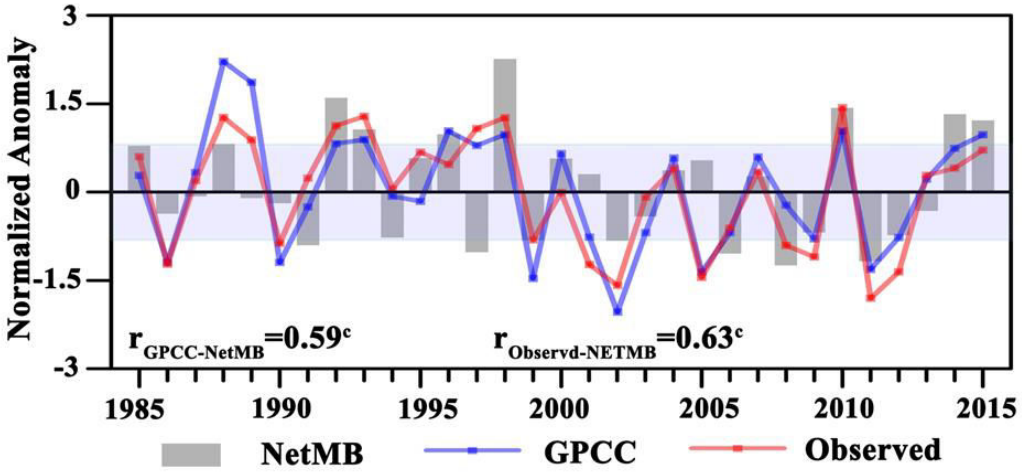


425

426 **Figure 9** The correlation between normalized southwest monsoon (SWM) rainfall
427 anomaly and net moisture budget (NetMB). The letter "c" shows a statistically significant
428 correlation at a 99% confidence level. The rainfall anomaly is calculated using station
429 observation (red line) and GPCC data product (blue line). The anomalous SWM rainfall
430 anomalies are above and below the shaded strip are considered as relatively wet and dry
431 SWM years, respectively.

432 In relatively wet SWM years, all months of the season showed positive anomalous
433 NetMB with respect to the long-term climatology, as shown in Figures 9a1-d1, where the
434 largest positive anomaly was observed in August ($1.40\times10^5$ kg $s^{-1}$) relative to the long-term
435 mean. However, the largest NetMB is observed in September ($6.00\times10^5$ kg $s^{-1}$), followed by
436 July ($5.73\times10^5$ kg $s^{-1}$), June ($4.52\times10^5$ kg $s^{-1}$), and August ($4.25\times10^5$ kg $s^{-1}$). Considering the
437 moisture influx via western boundary, positive anomalous net moisture influx is observed in
438 all the months except August, where the largest positive anomaly is recorded in July, which is
439 quite similar to an anomaly in September. On the other hand, the southern boundary showed
440 positive anomalous net moisture flux during all the months in the SWM season. With respect
441 to the long-term mean influx from the southern boundary, June ($0.07\times10^5$ kg $s^{-1}$)and July
442 ($0.77\times10^5$ kg $s^{-1}$) show the lowest and highest influx anomaly, respectively. The moisture
443 outflux from the eastern boundary shows a negative anomaly in June ($-0.08\times10^5$ kg $s^{-1}$) and

August ($-0.65\times10^5$ kg $s^{-1}$), while July ($0.55\times10^5$ kg $s^{-1}$) and September ($0.29\times10^5$ kg $s^{-1}$) showed a positive outflux anomaly during $SWM_{Wet}$ years. The northern boundary also acts as a moisture outflux boundary, where negative outflux anomalies are recorded all months except August ($0.29\times10^5$ kg $s^{-1}$).

In $SWM_{Dry}$ years, the long-term mean of NetMB for June, July, August, and September is $-0.31\times10^5$ kg $s^{-1}$, $-0.69\times10^5$ kg $s^{-1}$, $-0.32\times10^5$ kg $s^{-1}$, and $-0.15\times10^5$ kg $s^{-1}$, respectively (Figure 9a2-d2), which evident that all the months of the season showed below-average moisture availability. As a result of less moisture flux, the country receives below normal rainfall during the SWM season. Furthermore, we notice that the largest negative NetMB is recorded in July concerning its long-term mean (Figure 9b2) because moisture outflux from the eastern and southern boundary is stronger than moisture influx from eastern and northern boundaries. The moisture influx from the eastern boundary showed a positive anomaly for all months except July during $SWM_{Dry}$ years. It also shows that the first two months of the season have a below-average moisture influx from the southern boundary, but the next two months of the season have above-average moisture flux during $SWM_{Dry}$ years. During the $SWM_{Dry}$ years, the eastern and northern boundaries act as outflux boundaries where outfluxes are above average compared to their climatological mean except June. For instance, moisture outflux in September recorded the largest positive anomaly for both eastern ($1.17\times10^5$ kg $s^{-1}$) and northern ($0.53\times10^5$ kg $s^{-1}$) boundary compared to the rest of the months (Figure 9a2-d2).

### 3.5 Vertical Distribution of Moisture in Contrast Monsoon Years

According to Anderson et al. (2009), the role of low jet stream flow is critical in the moisture flux fluctuations and precipitation. For instance, Ordóñez et al. (2012) found that the Arabian Sea and the Indian Ocean, through the action of Somali Low-Level Jets, are the most

important source during the summer monsoon season. In particular, Malik et al. (2015) observe the largest moisture flux convergence at 925 hPa level in summer and at 850 hPa level in winter over central southwest Asia. Considering these facts, we also investigate the vertical distribution of regional moisture fluxes via each lateral boundaries for SWM seasons (Figure 10), where the climatology of moisture fluxes (shaded; Top x-axis) and the anomalous moisture fluxes in contrast monsoon years for each boundary are plotted (bottom x-axis). We found that the eastward total moisture influxes via western boundaries in the lower troposphere from the surface to 700 hPa was remarkably higher than the above 700 hPa levels. We observed positive anomalous moisture fluxes via the western boundary from 1000 to 700 hPa level (Figure 10a). After 700 hPa, negative anomalous moisture flux is reported to 450 hPa level. In contrast, the anomalous moisture influx from the western boundary at all the pressure levels are almost close to the zero lines, which indicates that the difference between the long-term mean an influx from $SWM_{Dry}$ is negligible (Figure 10a).

Compared to the western boundary, the southern boundary also acts as moisture input; however, the moisture influx via the southern boundary is smaller in magnitude (Figure 10c). According to the vertical structure of the southern boundary, moisture influx depicts large moisture transport from 1000 hPa to 700 hPa; afterward, it is gradually decreasing from 700

In the eastern boundary, the maximum moisture outflux is observed from 950 and 850 hPa levels, while it is gradually decreasing up to 450 hPa levels. In relatively wet monsoon years, the positive anomalous outflux is detected from the surface to 800 hPa level; afterward, the outflux anomaly becomes negative up to 450 hPa level. Interestingly we found that above-average moisture outflux from 1000 hPa to 500 hPa level during the $SWM_{Dry}$ years; meanwhile, the difference with the long-term average is not remarkable from 500 to 300 hPa levels (Figure 10b).

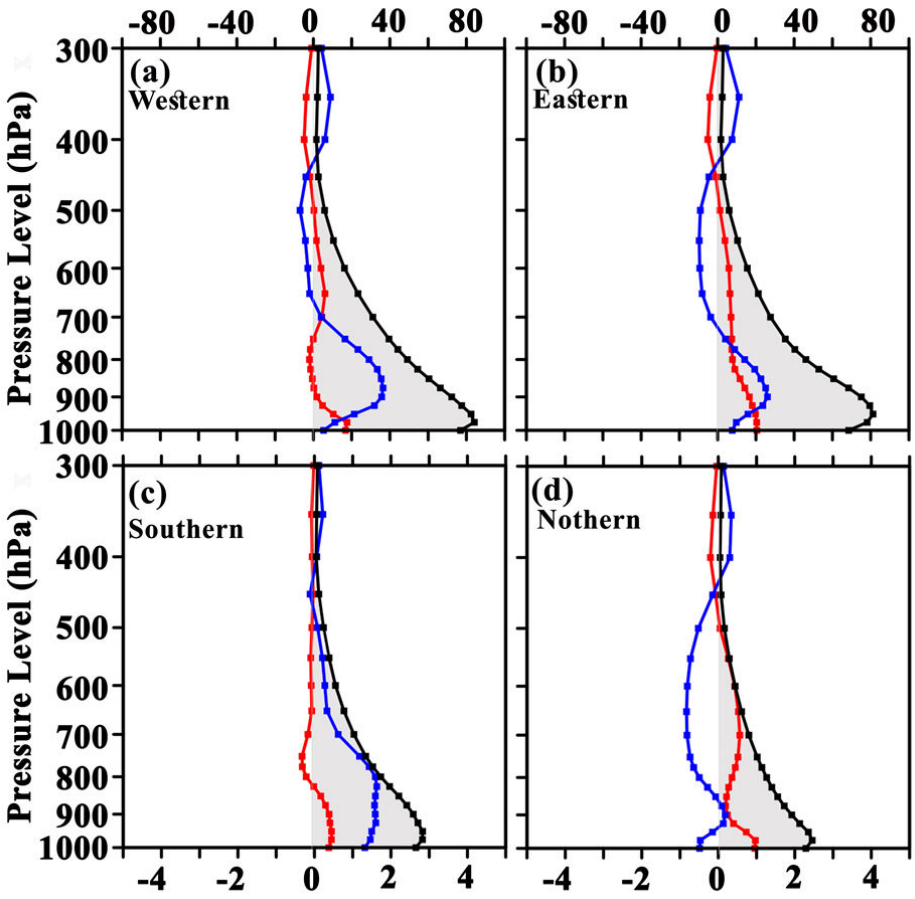


493

494 **Figure 10** Vertical distribution of the total water vapor flux (unit: $10^3$ $m^2s^{-1}$) via (a)
495 western boundary (6°N~10°N at 79.5°E) (b) eastern (6°N~10°N at 82°E), (c) southern
496 (79.5°E~82°E at 6°N) and (d) northern (79.5°E~ 82°E at 10° N) boundaries from the aspect
497 of climate mean (black line, x-axis at the top) and anomalous moisture flux (x-axis at the
498 bottom) in relatively wet (blue line) and relatively dry SWM (red line) southwest monsoon
499 (SWM) years.

500 As compared to moisture outflux from eastern boundaries, the moisture outflux via
501 northern boundaries is smaller in magnitude (Figure 10d). The northern boundaries depict
502 large moisture transport from 1000 hPa to 850 hPa, gradually decreasing from 700-300 hPa
503 levels. During $SWM_{Wet}$ years, negative anomalous outflux from the surface to the 450 hPa
504 level is dominant except for the 925-875 hPa level. In contrast, the positive outflux anomaly
505 is detected for the surface to 450 hPa during the $SWM_{Dry}$ years, which indicates that the

moisture outflux from the northern boundary is higher in $SWM_{Dry}$ years compared to the long-term mean of moisture outflux. This study revealed that the SWM rain in Sri Lanka also originated from the sea; mainly, a strong cross-equatorial low-level jet stream, with it is core close to the 850 hPa level over the Indian Ocean.

### 3.6 Moisture Fluxes Divergence in Contrast Monsoon Years

The available moisture in an area mainly depends on the moisture flux divergence/ convergence than the moisture fluxes, which only measures the moisture passing through the study domain (Wei et al. 2015). On the other hand, moisture flux convergence is more important for the probability of intensifying rainfall. Therefore, we made an attempt to investigate anomalous vertically integrated Total Moisture Flux Divergence (TMFD), Zonal Moisture Flux Divergence (ZMFD), and Meridional Moisture Flux Divergence (MMFD) over the total averaged area of Sri Lanka for contrast SWM years. Meanwhile, the long-term mean TMFD, ZMFD, and MMFD, and an anomaly of divergence component for each month of the season are calculated (Figures 9a-c). Notably, we found a negative anomalous TMFD ($–1.78\times10^{-5}$ kg $m^{-2}$ $s^{-1}$) in $SWM_{Wet}$ years compared to the long-term mean of TMFD ($–3.28\times10^{-5}$ kg $m^{-2}$ $s^{-1}$). In contrast, positive anomalous TMFD ($1.44\times10^{-5}$ kg $m^{-2}$ $s^{-1}$) is dominant for $SWM_{Dry}$ years (Figure 11a).

According to the monthly analysis, the long-term mean of TMFD in June, July, August, and September are $–3.31\times10^{-5}$, $–3.55\times10^{-5}$,$–2.99\times10^{-5}$, and $–3.2\times10^{-5}$ kg $m^{-2}$ $s^{-1}$, respectively. In $SWM_{Wet}$ years, we notice that all months in the SWM season show negative TMFD anomaly, while the lowest and highest TMFD anomaly is recorded in July ($–2.78\times10^{-5}$ kg $m^{-2}$ $s^{-1}$) and September ($–0.93\times10^{-5}$ kg $m^{-2}$ $s^{-1}$), respectively (Figure 11a). In contrast, all months of the season recorded positive TMFD anomalies during the $SWM_{Dry}$ years. For instance, the largest positive anomalous TMDF is recorded in June ($1.53\times10^{-5}$ kg $m^{-2}$ $s^{-1}$).

These findings suggest that negative TMFD may be more important for the heavier rainfall in the regions, while other factors, such as local topography conditions, may have a strong impact on localized rainfall during the SWM season. According to Wei et al. (2015), enhanced moisture flux convergence (–divergence) increases with precipitation intensity. Similarly, our result also suggests that above-average moisture convergence resulted in stong SWM rainfall. On the other hand, the below-average net moisture divergence caused rainfall subsidence during the SWM season, especially in $SWM_{Dry}$ years. In parallel with our findings, Lin and Shelton (2020) found the frequent occurrence of drought events during the SWM season since 2000 due to the net moisture divergence anomalies over Sri Lanka.

To identify the behavior of the zonal and meridional components of the TMFD in contrast SWM years, we further analyze ZMFD and MMFD separately (Figures 11b-c). Compared to the long-term average of the ZMFD in the SWM season ($-3.03 \times 10^{-5}$ kg $m^{-2}$ $s^{-1}$), the $SWM_{Wet}$ and $SWM_{Dry}$ years recorded negative ($-2.75\times10^{-5}$ kg $m^{-2}$ $s^{-1}$) and positive ($1.55\times10^{-5}$ kg $m^{-2}$ $s^{-1}$) anomalies, respectively. The long-term mean of the ZMFD in June ($-5.86\times10^{-5}$ kg $m^{-2}$ $s^{-1}$) and July ($-6.78\times10^{-5}$ kg $m^{-2}$ $s^{-1}$) is negative, while the next two months of the season depict positive ZMFD (Figure 11b). The results further show all the months of the SWM season have negative (positive) ZMFD anomalies in the $SWM_{Wet}$ ($SWM_{Dry}$) years. In $SWM_{Wet}$ years, the lowest negative ZMFD anomaly ($-3.24\times10^{-5}$ kg $m^{-2}$ $s^{-1}$) is observed in August, while September recorded the highest divergence ($-2.03\times10^{-5}$ kg $m^{-2}$ $s^{-1}$) compared to other months in the season (Figure 11b).

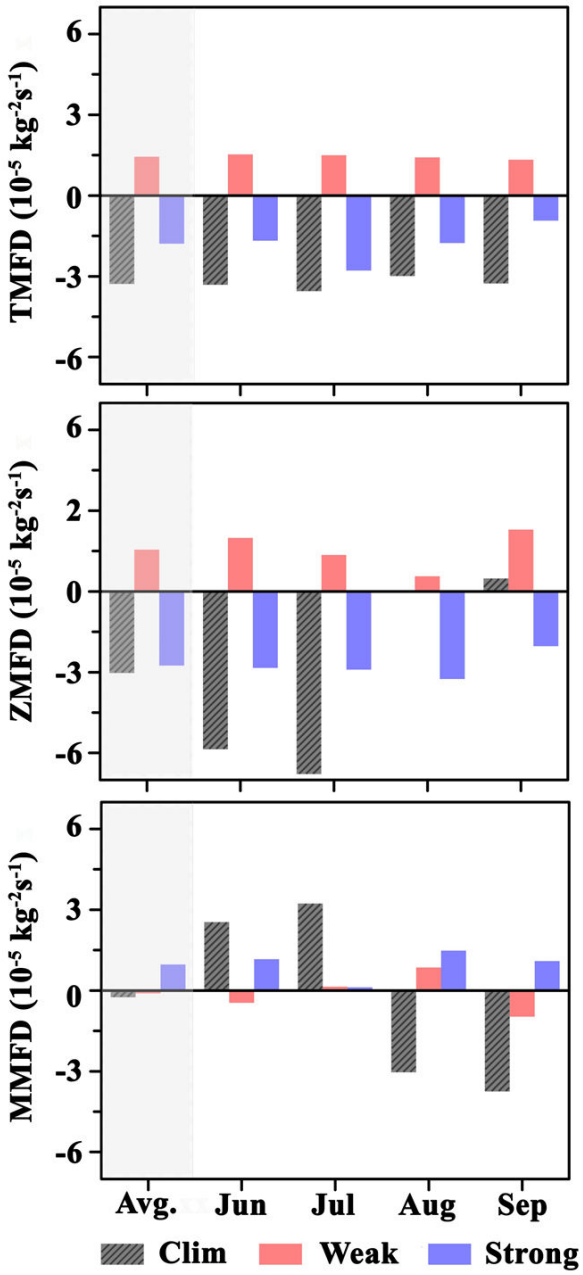


554

555

556 **Figure 11** The area-averaged (5.5°N~10°N, 80°E~82.5°E) seasonal and monthly
557 vertically integrated (a) Total Moisture Flux Divergence (TMFD), (b) Zonal Moisture Flux
558 Divergence (ZMFD) and Meridional Moisture Flux Divergence (MMFD) (units: $10^{-5}$ kg m$^{-2}$
559 s$^{-1}$) for (a) a long-term average of southwest (SWM) season, and anomalies for for relatively
560 (b) wet ($SWM_{Wet}$) and (c) dry SWM ($SWM_{Dry}$) years. The bars inside the shaded stip denote
561 the seasonal average climatology and anomalies in contrast SWM years.

562 The long term average of MMFD for SWM season is $-0.65\times10^{-5}$, while positive
563 ($0.96\times10^{-5}$ kg $m^{-2}$ $s^{-1}$) and negative ($-0.10\times10^{-5}$ kg $m^{-2}$ $s^{-1}$) anomalous MMFD is observed in
564 the $SWM_{wet}$ and $SWM_{Dry}$ years, respectively. We found that the June ($2.54\times10^{-5}$ kg $m^{-2}$ $s^{-1}$)
565 and July ($3.2\times10^{-5}$ kg $m^{-2}$ $s^{-1}$) showed strong MMFD, which become negative in August (–
566 $3.04\times10^{-5}$ kg $m^{-2}$ $s^{-1}$) and September ($-3.74\times10^{-5}$ kg $m^{-2}$ $s^{-1}$) as shown in Figure 11c. In
567 $SWM_{Wet}$ years, all the months recorded positive divergence anomaly, where the largest
568 positive anomaly ($1.48\times10^{-5}$ kg $m^{-2}$ $s^{-1}$) is recorded for August. During the $SWM_{Dry}$ years,
569 June ($-0.45\times10^{-5}$ kg $m^{-2}$ $s^{-1}$) and September ($-0.96\times10^{-5}$ kg $m^{-2}$ $s^{-1}$) show a negative MMFD
570 anomaly, while July ($0.14\times10^{-5}$ kg $m^{-2}$ $s^{-1}$) and August ($0.85\times10^{-5}$ kg $m^{-2}$ $s^{-1}$) report positive
571 MMFD (Figure 11c). The above results indicate inhomogeneity in the monthly TMFD,
572 ZMFD, and MMFD during the contrast SWM years, which characterizes the seasonal
573 average of them. Based on the long-term climatology, negative ZMFD components dominant
574 in the first two months of the SWM season, while the MMFD becomes negative in August
575 and September. Finally, we identified that the negative (positive) TMFD anomalies over Sri
576 Lanka could ascribe the above-average (below-average) rainfall in contrast SWM years.

577 ## 4 Discussion and Conclusion

578 It is noticed that around 60% of the terrestrial precipitation directly originates as a
579 result of moisture transported from the ocean (Gimeno et al. 2012) while excessive transports
580 are usually primary sources for extreme weather and flood events (Galarneau et al. 2010), as
581 well as interrupted transports, can lead to droughts and subsequent socioeconomic stresses.
582 Therefore a clear understanding of the mechanisms that force observed changes to the
583 hydrological cycle over Sri Lanka is crucial for water management and mitigate the
584 metrological induce disasters. Hence, the present study has been focused on finding out a
585 relationship between the variability of the oceanic moisture source and monsoon rainfall
586 (SWM) variability during relatively wet and dry monsoon years over Sri Lanka.

587 Based on the results, the cross-equatorial flux entering the west Indian Ocean from the
588 southern hemisphere is one of the most important sources of moisture for Sri Lanka during
589 the relatively wet monsoon SWM years. Furthermore, we noticed that the deficiency of
590 westerly moisture flux from the Arabian Sea results in below-average SWM rainfall over the
591 country. This study revealed that the Sri Lankan summer monsoon rain is also originated
592 from the sea; in particular, a strong cross-equatorial low-level jet stream, with it is core close
593 to the 850 hPa level over the Indian Ocean.

594 The vertically integrated moisture flux computation showed that the net positive
595 divergence over the western Indian Ocean and negative moisture flux divergence over Sri
596 Lanka, particularly, more negative VIMFD are concentrated to the west/southwest parts of
597 the country during the $SWM_{wet}$, which can ascribe why this region receives havier rainfall
598 during the SWM season. These positive moisture divergence developments were enhanced by
599 the strong westerly winds over the West Indian Ocean while abundant moisture was located
600 over Sri Lanka, which contributes to enhancing convection as well as cloud formation,
601 thunderstorms, and rainfall during the $SWM_{Wet}$ years. In contrast, the whole country showed
602 positive VIMFD during the relatively dry SWM years, which causes below-average SWM
603 rainfall over the country. This moisture transport analysis assists in explaining the occurrence
604 of extreme rainfall events in the SWM season in Sri Lanka; because many extreme rainfall
605 events originate with high moisture and an atmospheric disturbance. Interestingly, we found
606 below-average rainfall events after 2000 (6 events out of 9), which is resulted from the
607 observed weakening of the South Asian monsoon, which leads to lesser moisture transport
608 from the northwest Indian Ocean to Sri Lanka, with net moisture divergence anomalies (Lin
609 and Shelton 2020).

610 Previous studies (Pandey et al. 2019; Varikoden and Preethi 2013) suggest that sea
611 surface temperature also influences to enhancement and subsidence of SWM rainfall over

India. For instance, above-average (below-average) SWM rainfall occurred during the La Nina (El Nina) years over India. We also believe that SST over the Indian ocean and Pacific Ocene modulate relatively wet and dry SWM years. In future studies, we will investigate how SST changes and local evaporation affect the occurrence of above and below average SWM event in Sri Lanka

## Author Contributions

SS research conceptualization, methodology, formal analysis, data curation, writing original draft preparation, writing – review, and editing. All authors equally collaborated in the research presented in this publication by making the following contributions.


## Funding

This study was jointly supported by the CAS Strategic Priority Research Program (Grant No. XDA20060501), National Natural Science Foundation of China (41661144032), CAS The Belt, and Road Initiative Program (134111KYSB20160010), and China–Sri Lanka joint Center for Education and Research (CSL-CER).

## Acknowledgments

We are thankful to the Meteorological Department, Sri Lanka, for providing weather data. SS acknowledged the CAS–TWAS President's Fellowship Program for International Ph.D. student and Industrial Technology Institute–Sri Lanka for their supports.


**Conflicts of Interest**: The author reported no potential conflict of interest.

## Availability of data and material

The datasets generated during and/or analysed during the current study are available from the corresponding author on reasonable request.

## Code availability

The codes used during the current study are not available.

## Ethics approval

Disclosure of potential conflicts of interest

## Consent to participate

Not applicable

## Consent for publication (

Not applicable

## References


Allan RP, Soden BJ (2007) Large discrepancy between observed and simulated precipitation trends in the ascending and descending branches of the tropical circulation Geophysical Research Letters 34:L18705 doi:https://doi.org/10.1029/2007GL031460

Anderson B, Ruane A, Roads J, Kanamitsu M (2009) Estimating the Influence of Evaporation and Moisture-Flux Convergence upon Seasonal Precipitation Rates. Part II: An Analysis for North America Based upon the NCEP–DOE Reanalysis II Model Journal of Hydrometeorology 10:893–911 doi:https://doi.org/10.1175/2009JHM1063.1

Dar SS, Ghosh P (2017) Estimates of land and sea moisture contributions to the monsoonal rain over Kolkata, deduced based on isotopic analysis of rainwater Earth Syst Dynam 8:313-321 doi:https://doi.org/10.5194/esd-8-313-2017

Dee DP et al. (2011) The ERA-Interim reanalysis: configuration and performance of the data assimilation system Quarterly Journal of the Royal Meteorological Society 137:553-597 doi:https://doi.org/10.1002/qj.828

Galarneau TJ, Bosart LF, Schumacher RS (2010) Predecessor Rain Events ahead of Tropical Cyclones Monthly Weather Review 138:3272-3297 doi:https://doi.org/10.1175/2010mwr3243.1

Gao Q, Sun Y (2016) Changes in water vapor transport during the Meiyu season after 2000 and their relationship with the Indian ocean SST and Pacific-Japan pattern Dynamics of Atmospheres and Oceans 76:141-153 doi:http://dx.doi.org/10.1016/j.dynatmoce.2016.10.006

Gimeno L et al. (2016) Major Mechanisms of Atmospheric Moisture Transport and their Role in Extreme Precipitation Events Annual Review of Environment and Resources 3:1-25 doi:https://doi.org/10.1146/annurev-environ-110615-085558

Gimeno L et al. (2012) Oceanic and terrestrial sources of continental precipitation Reviews of Geophysics 50:RG4003 doi:https://doi.org/10.1029/2012RG000389

Held IM, Soden BJ (2006) Robust Responses of the Hydrological Cycle to Global Warming Journal of Climate 19:5686-5699 doi:https://doi.org/10.1175/jcli3990.1

Joseph P, Simon A (2005) Weakening trend of the southwest monsoon current through peninsular India from 1950 to the present CURRENT SCIENCE 89:687-694

Joseph PV, Sijikumar S (2004) Intraseasonal Variability of the Low-Level Jet Stream of the Asian Summer Monsoon Journal of Climate 17:1449-1458 doi:https://doi.org/10.1175/1520-0442(2004)017<1449:IVOTLJ>2.0.CO;2

Kathayat G et al. (2016) Indian monsoon variability on millennial-orbital timescales Scientific Reports 6:24374 doi:https://doi.org/10.1038/srep24374

Konwar M, Parekh A, Goswami BN (2012) Dynamics of east-west asymmetry of Indian summer monsoon rainfall trends in recent decades Geophysical Research Letters 39:L10708 doi:https://doi.org/10.1029/2012GL052018

Levine RC, Turner AG (2012) Dependence of Indian monsoon rainfall on moisture fluxes across the Arabian Sea and the impact of coupled model sea surface temperature biases Climate Dynamics 38:2167-2190 doi:https://doi.org/10.1007/s00382-011-1096-z

Limin S, Oue H, Takase K (2015) Estimation of Areal Average Rainfall in the Mountainous Kamo River Watershed, Japan Journal of Agricultural Meteorology 71:90-97 doi:https://doi.org/10.2480/agrmet.D-14-00055

Lin Z, Shelton S (2020) Interdecadal Change of Drought Characteristics in Mahaweli River Basin of Sri Lanka and the Associated Atmospheric Circulation Difference Front Earth Sci 8:306-324 doi:https://doi.org/10.3389/feart.2020.00306

Liu B, Tan X, Gan TY, Chen X, Lin K, Lu M, Liu Z (2020) Global atmospheric moisture transport associated with precipitation extremes: Mechanisms and climate change impacts WIREs Water 7:e1412 doi:https://doi.org/10.1002/wat2.1412

Malik KM, Taylor PA, Szeto K (2015) Characteristics of moisture flux convergence in Central Southwest Asia Theoretical and Applied Climatology 120:643-659 doi:https://doi.org/10.1007/s00704-014-1192-1

699 Malmgren BA, Hulugalla R, Hayashi Y, Mikami T (2003) Precipitation trends in Sri Lanka
700 since the 1870s and relationships to El Niño–southern oscillation International Journal
701 of Climatology 23:1235-1252 doi:https://doi.org/10.1002/joc.921
702 Marambe B et al. (2015) Climate, Climate Risk, and Food Security in Sri Lanka: Need for
703 Strengthening Adaptation Strategies. doi:https://doi.org/10.1007/978-3-642-38670-
704 1_120
705 Neiman PJ, Ralph FM, Moore BJ, Hughes M, Mahoney KM, Cordeira JM, Dettinger MD
706 (2013) The Landfall and Inland Penetration of a Flood-Producing Atmospheric River
707 in Arizona. Part I: Observed Synoptic-Scale, Orographic, and Hydrometeorological
708 Characteristics Journal of Hydrometeorology 14:460-484
709 doi:https://doi.org/10.1175/jhm-d-12-0101.1
710 O'Gorman PA (2015) Precipitation Extremes Under Climate Change Current Climate
711 Change Reports 1:49-59 doi:https://doi.org/10.1007/s40641-015-0009-3
712 Ordóñez P, Ribera P, Gallego D, Peña-Ortiz C (2012) Major moisture sources for Western
713 and Southern India and their role on synoptic-scale rainfall events Hydrological
714 Processes 26:3886-3895 doi:https://doi.org/10.1002/hyp.8455
715 Pandey V, Misra AK, Yadav SB (2019) Impact of El-Nino and La-Nina on Indian Climate
716 and Crop Production. In: Sheraz Mahdi S (ed) Climate Change and Agriculture in
717 India: Impact and Adaptation. Springer International Publishing, Cham, pp 11-20.
718 doi:10.1007/978-3-319-90086-5_2
719 Pathak A, Ghosh S, Kumar P, Murtugudde R (2017) Role of Oceanic and Terrestrial
720 Atmospheric Moisture Sources in Intraseasonal Variability of Indian Summer
721 Monsoon Rainfall Scientific Reports 7:12729 doi:https://doi.org/10.1038/s41598-017-
722 13115-7
723 Rajeevan M, Bhate J, Jaswal AK (2008) Analysis of variability and trends of extreme rainfall
724 events over India using 104 years of gridded daily rainfall data Geophysical Research
725 Letters 35 doi:https://doi.org/10.1029/2008gl035143
726 Ranatunge E, Malmgren BA, Hayashi Y, Mikami T, Morishima W, Yokozawa M, Nishimori
727 M (2003) Changes in the Southwest Monsoon mean daily rainfall intensity in Sri
728 Lanka: relationship to the El Nino-Southern Oscillation Palaeogeogr Palaeocl 197:1-
729 14 doi:https://doi.org/10.1016/S0031-0182(03)00383-3
730 Ratna SB, A.Cherchi, Joseph PV, Behera S, Abish B, Masina S (2014) Moisture trend over
731 the Arabian Sea and its influence on the indian summer monsoon precipitation. vol
732 225. Centro Euro-Mediterraneo per i Cambiamenti Climatici, Lecce, Italy

733 Ratna SB, Cherchi A, Joseph PV, Behera SK, Abish B, Masina S (2016) Moisture variability
734 over the Indo-Pacific region and its influence on the Indian summer monsoon rainfall
735 Climate Dynamics 46:949-965 doi:https://doi.org/10.1007/s00382-015-2624-z
736 Rayner D, Chen D (2010) Extreme rainfall events in southern Sweden: where does the
737 moisture come from? AU - Gustafsson, Malin Tellus A: Dynamic Meteorology and
738 Oceanography 62:605-616 doi:https://doi.org/10.1111/j.1600-0870.2010.00456.x
739 Roxy MK et al. (2017) A threefold rise in widespread extreme rain events over central India
740 Nature communications 8:708-708 doi:https://doi.org/10.1038/s41467-017-00744-9
741 Rubasinghe R, Gunatilake SK, Chandrajith R (2015) Geochemical characteristics of
742 groundwater in different climatic zones of Sri Lanka Environmental Earth Sciences
743 74:3067-3076 doi:https://doi.org/10.1007/s12665-015-4339-1
744 Schneider U, Becker A, Finger P, Meyer-Christoffer A, Rudolf B, Ziese M (2011) GPCC full
745 data reanalysis version 6.0 at 0.5°: Monthly land-surface precipitation from rain-
746 gauges built on GTS-based and historic data Deutscher Wetterdienst
747 doi:https://doi.org/10.5676/DWD_GPCC/FD_M_V6_050
748 Shashikanth K, Salvi K, Ghosh S, Rajendran K (2014) Do CMIP5 simulations of Indian
749 summer monsoon rainfall differ from those of CMIP3? Atmospheric Science Letters
750 15:79-85 doi:https://doi.org/10.1002/asl2.466
751 Shelton S, Lin Z (2019) Streamflow variability over the Period of 1990–2014 in Mahaweli
752 River basin, Sri Lanka and Its Possible Mechanisms Water 11:2485-2506 doi:
753 https://doi.org/10.3390/w11122485
754 Trenberth KE (1999) Conceptual Framework for Changes of Extremes of the Hydrological
755 Cycle With Climate Change. In: Karl TR, Nicholls N, Ghazi A (eds) Weather and
756 Climate Extremes: Changes, Variations and a Perspective from the Insurance
757 Industry. Springer Netherlands, Dordrecht, pp 327-339.
758 doi:https://doi.org/10.1007/978-94-015-9265-9_18
759 Trenberth KE, Dai A, Rasmussen RM, Parsons DB (2003) The Changing Character of
760 Precipitation Bulletin of the American Meteorological Society 84:1205-1217
761 doi:https://doi.org/10.1175/bams-84-9-1205
762 Trenberth KE, Guillemot CJ (1998) Evaluation of the atmospheric moisture and hydrological
763 cycle in the NCEP/NCAR reanalyses Climate Dynamics 14:213-231
764 doi:https://doi.org/10.1007/s003820050219
765 Turner AG, Annamalai H (2012) Climate change and the South Asian summer monsoon
766 Nature Clim Change 2:587-595 doi:https://doi.org/10.1038/nclimate1495

Ullah K, Gao S (2012) Moisture transport over the Arabian Sea associated with summer rainfall over Pakistan in 1994 and 2002 Advances in Atmospheric Sciences 29:501-508 doi:http://dx.doi.org/10.1007/s00376-011-0200-y

Varikoden H, Preethi B (2013) Wet and dry years of Indian summer monsoon and its relation with Indo-Pacific sea surface temperatures International Journal of Climatology 33:1761-1771 doi:10.1002/joc.3547

Wang Z et al. (2017) Does drought in China show a significant decreasing trend from 1961 to 2009? Science of The Total Environment 579:314-324 doi:https://doi.org/10.1016/j.scitotenv.2016.11.098

Wasko C, Lu WT, Mehrotra R (2018) Relationship of extreme precipitation, dry-bulb temperature, and dew point temperature across Australia Environmental Research Letters 13:074031 doi:https://doi.org/10.1088/1748-9326/aad135

Wei J, Su H, Yang Z-L (2015) Impact of moisture flux convergence and soil moisture on precipitation: A case study for the southern United States with implications for the globe Climate Dynamics 46 doi:https://doi.org/10.1007/s00382-015-2593-2

Xavier A, Kottayil A, Mohanakumar K, Xavier PK (2018) The role of monsoon low-level jet in modulating heavy rainfall events International Journal of Climatology 38:e569-e576 doi:https://doi.org/10.1002/joc.5390

786